An Electrochemical Study on Anion Doping-Undoping Process of Polyacetylene by Means of FFT Impedance Measurement

Tetsuya Osaka* and Takashi Kitai
Department of Applied Chemistry, School of Science and Engineering, Waseda University, Okubo, Shinjuku-ku, Tokyo 160

(Received June 27, 1983)

An electrochemical anion doping-undoping process of *cis*-polyacetylene, $(CH)_x$, was investigated in 1 mol dm^{-3} $LiClO_4$ or $LiBF_4$ in propylene carbonate by the FFT impedance measurement. This could be applied to the system with time-variation because of its high speed measuring duration. The doping-undoping process of the anion was represented by the Randles-type equivalent circuit, considering the corrective term concerned with surface roughness. The impedance behavior of the doping-undoping process was pursued by the variation of resistive component, *Rr*. The value of *Rr* was mainly reflected by the dopant concentration at the surface. The variation of *Rr* indicated that rapid or strong-drive doping produces non-uniformity of dopant distribution in the film and high dopant concentration at the surface.

A conduction polymer has recently been developed as a new electrode material for high-density batteries. Polyacetylene, $(CH)_x$, is very suitable as a new electrode material, since its conductivity can be varied over twelve orders of magnitude depending on the dopant concentration[1] and it can be easily synthesized. Polyacetylene can be electrochemically doped as either n-type or p-type to induce semiconducting and ultimately metallic conditions with a variety of species.[2,3] Accordingly, some attempts have been made to use polyacetylene as an electrode material in lightweight rechargeable storage batteries.[4,5] Studies of the electrochemical characteristics of polyacetylene, however, are recent and so far there have been only a few reports on the analysis of the electrochemical doping or undoping process of polyacetylene.[6] In this paper, we report the electrochemical doping-undoping process of polyacetylene as a cathode by means of electrochemical measurements, especially the FFT impedance method.[7] The FFT impedance method has an advantage of rapid measurement for the frequency-dispersion within a very short time-duration. Phenomena with time-variation such as the doping-undoping process may be analyzed easily by this method.

Experimental

The *cis*-polyacetylene films with 0.3 mm thickness were prepared by the Shirakawa method.[8] The working electrode consisted of a single circular film of 8 mmϕ of the *cis*-$(CH)_x$ (weight density 0.44 g cm^{-3}), attached to a platinum plate as a current collector. A circular platinum or lithium mounted on platinum counter electrode was placed opposite to the *cis*-$(CH)_x$ working electrode in a Teflon or glass cell. A Li/Li^+, reference electrode was set at the mid point between the working and counter electrodes, and the potential was referred to the Li/Li^+ in the same solution. The electrolyte solution was 1.0 mol dm^{-3} $LiClO_4$ or 1.0 mol dm^{-3} $LiBF_4$ in propylene carbonate (PC). The solvent and electrolyte were purified and handled in the usual method.[4,9] Electrochemical measurements were performed by voltammetry and the FFT impedance method with frequency range between 0.01 and 2.5 kHz. The system and method for the FFT impedance measurements were the same as described in the previous paper.[7] All experiments were carried out in a dry and inert Ar gas atmosphere.

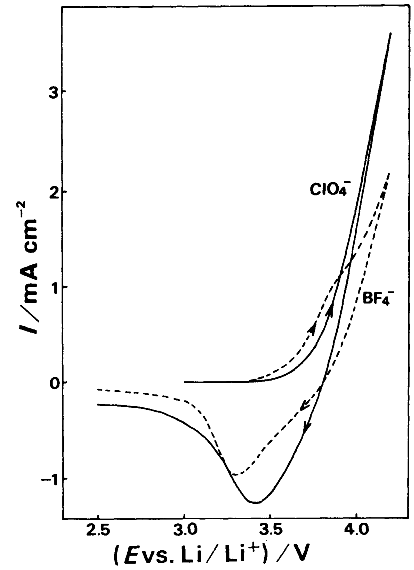

Fig. 1. Current *vs.* potential curves of $(CH)_x$ electrode at anion doping-undoping process in various solutions at 1 mV s^{-1} at Ar atmosphere.
——: 1 mol dm^{-3} $LiClO_4$/PC, ----: 1 mol dm^{-3} $LiBF_4$/PC.

Results and Discussion

Current vs. *Potential Curves of* $(CH)_x$ *Electrode.* Figure 1 shows the typical current *vs.* potential curves of the $(CH)_x$ electrode at the third time scan for the anion doping-undoping process in 1 mol dm^{-3} $LiClO_4$/PC and 1 mol dm^{-3} $LiBF_4$/PC using a scan rate of 1 mV s^{-1}, since the behavior of current *vs.* potential curves with 1 mV s^{-1} becomes steady-state from the third time scan. The first time scan showed the greatest difference from the steady-state of the current *vs.* potential curve, *i.e.*, the doping at the first time scan was small. In Fig. 1, the anodic current indicates anion doping into $(CH)_x$ and the cathodic current indicates anion undoping from doped $(CH)_x$, respectively. The electrochemical doping reaction involves the partial oxidation of $(CH)_x$ as shown in Eq. 1.[3,5]

$$(CH)_x + xyClO_4^- \longrightarrow [(CH^{+y})(ClO_4)_y^-]_x + xye. \quad (1)$$

The $(CH)_x$ film is doped readily to the composition of $[CH(ClO_4)_y]_x$ or $[CH(BF_4)_y]_x$ from approximately the same potential around 3.4 V in each electrolyte solution. The anodic doping current increases more rapidly for ClO$_4^-$ doping than for BF$_4^-$ doping, though at the initial doping potential the increase for BF$_4^-$ anion is greater than that for ClO$_4^-$ anion. In Fig. 1, the charging ratio from anodic scan until the anodic current becoming zero at cathodic scan was 1.47% for ClO$_4^-$ and 0.72% for BF$_4^-$, respectively.[†] At the cathodic scan, the cathodic currents for the undoping process show a peak at 3.4 V for ClO$_4^-$ undoping and at 3.3 V for BF$_4^-$ undoping. It is assumed from the behavior of the current-potential curves that ClO$_4^-$ anion doping-undoping occurs easier than BF$_4^-$ anion doping-undoping. The doping process as seen in Eq. 1 shows that the doped polymer is utilized as a cathode material, and the characteristics of doping-undoping process for ClO$_4^-$ may be superior to that for BF$_4^-$, thus the polyacetylene doped ClO$_4^-$ anion might be a superior cathode for a high power density battery of (CH)$_x$.

Impedance Measurements of the (CH)$_x$ Electrode. Figures 2(a) and 2(b) show the impedance of the (CH)$_x$ electrode at various potentials in 1 mol dm^{-3} LiBF$_4$/PC during anodic and cathodic scans, respectively, at 1 mV s^{-1}. At the anodic scan in Fig. 2(a), the impedance plots are semi-circles, and their diameters decrease with the doping process. The behavior of the cathodic scan for the undoping process is also similar to that of the anodic scan as seen in Fig. 2(b), and the diameters increase with the undoping process. Figure 3 shows the impedance representation of (CH)$_x$ in 1 mol dm^{-3} LiClO$_4$/PC at various doping levels using potential-step doping. The doping potentials for p-(CH)$_x$ are 3.6, 3.8, and 4.0 V for Figs. 3(a)—(c), respectively. The behavior shown in Fig. 3 is similar to that in Fig. 2(a) for the potential-scaning doping process. However, the greater the anodic potential of the doping level becomes, the earlier the diameter of semi-circle becomes small, namely, the diameter of semi-circle is shorter even at the same charging value when the doping is performed at the more anodic potential. This behavior is shown more clearly in Fig. 5. The impedance representation of (CH)$_x$ for ClO$_4^-$ anion doping-undoping process is similar to that for BF$_4^-$.

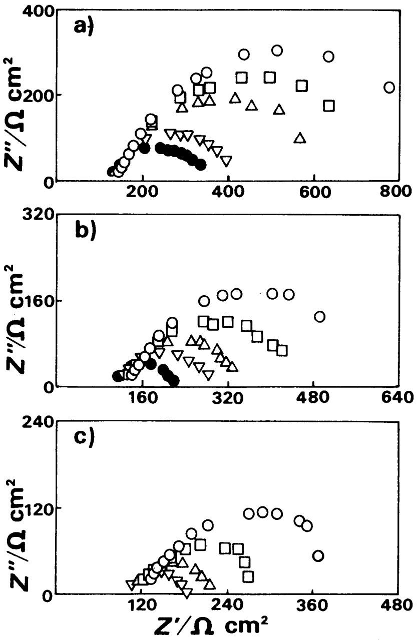

Fig. 3. Impedance representations of (CH)$_x$ electrode at anion doping process with using potential-step in 1 mol dm^{-3} LiBF$_4$/PC at Ar atmosphere.
a) Doping at constant potential of 3.6 V at various charges; ○: 0.2 mC, □: 3.4 mC, △: 10.4 mC, ▽: 44.0 mC, ●: 70.0 mC. b) Doping at constant potential of 3.8 V at various charges; ○: 0.4 mC, □: 11.0 mC, △: 30.0 mC, ▽: 50.0 mC, ●: 90.0 mC. c) Doping at constant potential of 4.0 V at various charges; ○: 1.2 mC, □: 19.6 mC, △: 56.6 mC, ▽: 96.0 mC.

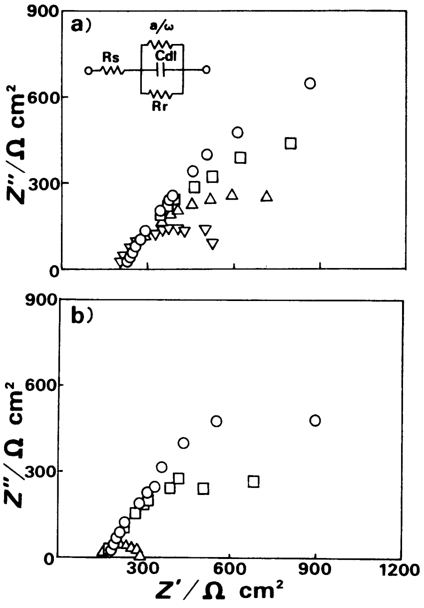

Fig. 2. Impedance representations of (CH)$_x$ electrode at anion doping-undoping process with using potential-sweep at 1 mV s^{-1} in 1 mol dm^{-3} LiBF$_4$/PC at Ar atmosphere.
a) Doping process measured at various potentials; ○: 3.5 V, □: 3.6 V, △: 3.7 V, ▽: 3.8 V. b) Undoping process measured at various potentials; ○: 3.0 V, □: 3.15 V, △: 3.3 V.

The theoretical equivalent circuit for the analysis and the interpretation of the experimental data shown in Fig. 2 are described as follows. The doping-undoping results are interpreted by the Randles-type equivalent circuit shown in Fig. 2(a), which displays a semi-circle in the impedance representation. The components of *Rs, Rr, Cdl,* and $a\,\omega^{-1}$, (ω: angular frequency) are the solution resistance, the resistive component due to the electrode reaction, the double-layer capacitance, and the corrective term concerned with surface roughness.[10] The surface of polyacetylene film may be porous because of it being composed of a fibril unit, thus the term concerned with the roughness, $a\,\omega^{-1}$, should be added into the circuit. If porous states are assumed, the double-layer capacitance, *Cdl,* means the total value of each pore's double-layer capacitance. The resistive component, *Rr,* arises

---

[†] Here, 1% doping corresponds to 278 mC.

mainly from two factors of the partial oxidation or reduction (*i.e.*, doping-undoping) reaction and of the film resistivity itself. The diffusion of the anion into the film (or diffusion of anion from exterior to interior of fibrils) is not directly detected between these frequency regions as seen in Fig. 2. The double-layer capacitance, *Cdl*, of $(CH)_x$ shows the same value of *ca.* 8.0 $\mu F\,cm^{-2}$ as that of the platinum electrode and also the value of *Cdl* is scarcely changed by the doping-undoping process. The value of the term '*a*' is very large and it is scarcely changed by the doping-undoping process. This means that the semi-circle is hardly inclined from the real component axis as is seen in Fig. 2. Accordingly, the information from the values of *Cdl* and '*a*' suggests that the surface porosity scarcely influences the impedance behavior of the polyacetylene film. This conclusion may be due to the very fine porosity of the $(CH)_x$ film (of the order of ten nm) formed by the fibril unit. A slight variation of *Rs* was observed in Figs. 2 and 3; this can be caused by the swelling of the $(CH)_x$ film on doping, which causes a decrease of the distance between the electrodes.[††] The value of *Rr*, which corresponds to the diameter of the semi-circle, changes greatly during the doping-undoping process. The value of *Rr* decreases with doping, while it increases with undoping. Consequently, the values of *Rs, Cdl*, and '*a*' are scarcely changed by the doping-undoping process but the opposite is true for *Rr*. Accordingly, there is a high possibility that the doping-undoping process of $(CH)_x$ is associated with the variation of *Rr*.

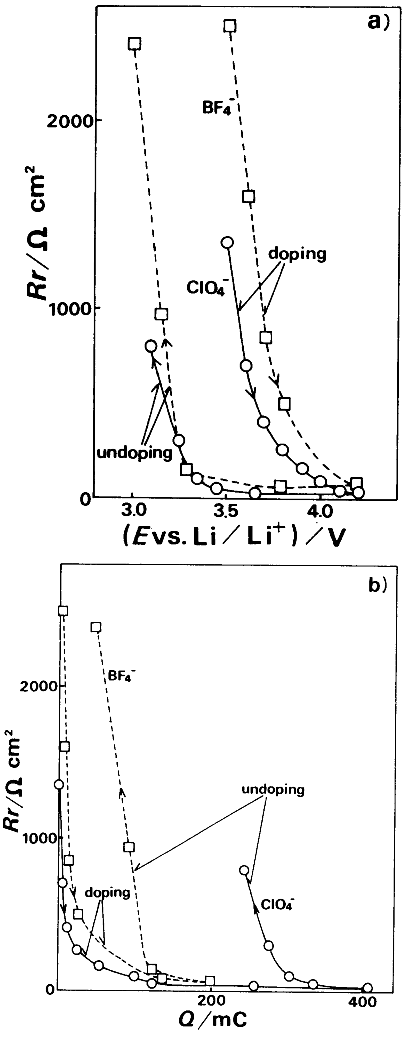

Fig. 4. Variation of resistive component, *Rr*, in equivalent circuit as a function of potential, *E*, (Fig. 4(a)) or amount of charge, *Q*, (Fig. 4(b)) of $(CH)_x$ electrode at anion doping-undoping process with using scaning at 1 $mV\,s^{-1}$ in various solutions.
○: 1 $mol\,dm^{-3}$ $LiClO_4$/PC, □: 1 $mol\,dm^{-3}$ $LiBF_4$/PC.

Variation of Rr Value of $(CH)_x$ *at Doping-Undoping Process.* Figure 4(a) shows the variation of the *Rr* value of the $(CH)_x$ electrode as a function of the potential during the potential-sweep doping-undoping process with 1 mV s^{-1} in the two kinds of solution. In both solutions of $LiClO_4$ and $LiBF_4$ in propylene carbonate, the value of *Rr* greatly decreases at the initial doping potential and finally reaches a small constant value. During the undoping scan, the value of *Rr* increases with the undoping process. The decrease of *Rr* for ClO_4^- ion is larger than that for BF_4^- ion at the same doping potential. At the beginning of the cathodic scan, an anodic current is observed until 3.8 V in the current *vs.* potential curves in Fig. 1. From the potential of 3.8 V during cathodic scan, anion undoping starts to occur and the values of *Rr* begins to increase abruptly at *ca.* 3.3 V after sufficient undoping process. A similar variation of *Rr* is observed in both scans and in both solutions, but during the anion doping process, the value of *Rr* for ClO_4^- doping is always smaller than that of BF_4^- doping at the same potential. This indicates that a greater amount of ClO_4^- anion is doped at the same potential and that the ClO_4^- anion can be doped more easily than the BF_4^- anion.[**] Since the measured impedance reflects the value not at the whole impedance of polyacetylene film electrode but at the interface between film electrode and solution, the variation of *Rr* is assumed to correspond to that at the surface region of $(CH)_x$ and the electrode reaction at the interface. The value of *Rr* is considered to contain two factors (i) the reaction resistance for the doping-undoping process at the interface as shown in Eq. 1 and (ii) the film resistivity of the $(CH)_x$ film itself at the actual surface region. The main factor related to the abrupt variation of *Rr* is more probably the latter than the former, because the former is usually not more than one hundred ohms. The variation of *Rr* can also be represented as a function of the amount of charge doped as seen in Fig. 4(b). In Fig. 4(b), the value of *Rr* decreases abruptly with the increase in the amount of charge, *Q*, especially at the beginning of the doping process, and it becomes constant after 100 mC.

[††] The cell used has the volume of 0.283 cm^3 for electrolyte solution and the distance between working and reference electrodes is 0.58 cm. The swelling of $(CH)_x$ film is observed *ca.* 0.2 cm at the most, which may cause the decrease of *Rs* *ca.* 30%.

[**] The Stokes' radii of ClO_4^- and BF_4^- ions in PC were reported as 0.31 and 0.28 nm, respectively.[11] Thus, the above results cannot simply be explained by the radii of ions. The ease of doping in the $(CH)_x$ film might be discussed by considering the interaction between the dopant ions and $(CH)_x$ or other factors.

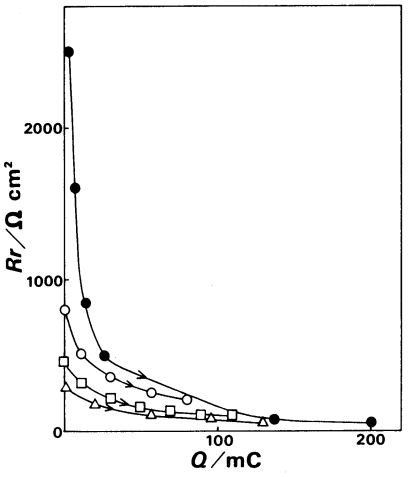

Fig. 5. Variation of resistive component, *Rr*, in equivalent circuit as a function of amount of charge of $(CH)_x$ electrode at anion doping-undoping process with using potential-step at various potentials in 1 mol dm^{-3} $LiClO_4$/PC.
○: 3.6 V, □: 3.8 V, △: 4.0 V, ●: potential-sweep doping at 1 mV s^{-1}.

On the other hand, the value of *Rr* increases with the decrease in *Q*, and the abrupt increase starts from a different point of the fairly doped amount of charge. This can be explained by the fact that the dopant anions entered deeply into the fibrils from the film surface but can not get out of them so easily. These results also strongly indicate that the variation of *Rr* does not reflect the total dopant concentration but only the dopant concentration at the surface of the $(CH)_x$ film. The hysteresis in the potential *vs*. charge relation similar to that in Fig. 4(b) has already been noted and discussed.[5,12,13] The hysteresis can be explained more readily by the variation of *Rr* as seen in Fig. 4(b).

Figure 5 shows the relationship between *Rr* and *Q* for the anion doping process by various doping methods in 1 mol dm^{-3} $LiBF_4$/PC In Fig. 5, the value of *Rr* at the potential-sweep doping with 1 mV s^{-1} is always larger than that at the potential-step doping. During the potential-step doping the value of *Rr* is decreased to less values by the very small charge of several mC's at the initial doping stage as compared with that during the potential-sweep doping. Moreover, the decrease of *Rr* occurs earlier at more anodic potential doping even for the same amount of charge doped. In the case of the potential-sweep doping with 1 mV s^{-1}, the doping rate is slower as compared with that of the potential-step doping. Then, the anion dopant diffuses more readily into the interior of the polyacetylene film. It is expected that the dopant concentration at the surface of the film is higher for the faster or stronger doping process. This assumption can readily explain the different variation of *Rr* by the different doping method. A similar behavior was observed also in 1 mol dm^{-3} $LiClO_4$/PC.

In conclusion, the resistive component, *Rr*, in the equivalent circuit reflects the dopant concentration at the surface of the film and the doped conditions can be detected by the variation of *Rr*. Rapid doping produces non-uniform dopant conditions of the surface concentration of dopant being very high. These non-uniformed states of the dopant cause the decrease of *Rr* and they tend to make the film potential more anodic.

The authors are indebted to Mr. Yoshimitsu Sawada, Showa Denko Co. Ltd., for providing polyacetylene samples and for helpful discussion.

References

1) C. K. Chiang, S. C. Gau, C. R. Fincher Jr., Y. W. Park, A. G. MacDiarmid, and A. J. Heeger, *Appl. Phys. Lett.*, **33**, 18 (1978).

2) P. J. Nigrey, A. G. MacDiarmid, and A. J. Heeger, *J. Chem. Soc., Chem. Commun.*, **1979**, 594.

3) D. Maclnnes Jr., M. A. Druy, P. J. Nigrey, D. P. Nairns, A. G. MacDiarmid, and A. J. Heeger, *J. Chem. Soc., Chem. Commun.*, **1981**, 317.

4) P. J. Nigrey, D. Maclnnes Jr., D. P. Nairns, and A. G. MacDiarmid, *J. Electrochem. Soc.*, **128**, 1651 (1981).

5) K. Kaneto, M. Maxfield, D. P. Nairns, and A. G. MacDiarmid, *J. Chem. Soc., Faraday Trans. 1*, **78**, 3417 (1982).

6) M. Aizawa, H. Shinohara, and H. Shirakawa, *Polym. Prepr. Jpn*, **31**, 2815 (1982); M. Aizawa, H. Shinohara, and S. Watanabe, 46th National Meeting of the Chem. Soc. Jpn., Niigata, October 1982, Abstract, p. 132; M. Aizawa, H. Shinohara, S. Watanabe, and H. Shirakawa, 49th Conference of Electrochem. Soc. Jpn., Extended Abstract, p. 155 (1982).

7) T. Osaka, and K. Naoi, *Bull. Chem. Soc. Jpn.*, **55**, 36 (1982).

8) T. Ito, H. Shirakawa, and S. Ikeda, *J. Polym. Sci.*, **12**, 11 (1974).

9) Y. Matsuda, *Denki Kagaku*, **48**, 665 (1980).

10) R. J. Brodd, *J. Res. Natl. Bur. Stand., Sect. A*: **65**, 275 (1961).

11) Y. Matsuda, H. Nakashima, M. Morita. and Y. Takasu, *J . Electrochem. Soc.*, **128**, 2552 (1981).

12) A. Feldblum, J. H. Kaufman, S. Etemad, A. J. Heeger, T. C. Chung, and A. G. MacDiarmid, *Phys. Rev. B*, **26**, 815 (1982).

13) J. H. Kaufman, J. W. Kaufer, A. J. Heeger, R. Kaner, and A. G. MacDiarmid, *Phys. Rev. B.*, **26**, 2327 (1982).